Waste Management 186 (2024) 318–330

Contents lists available at ScienceDirect

Waste Management

journal homepage: www.elsevier.com/locate/wasman

Research Paper

Climate impacts of landfill gas emissions: Analysis for 20-year and 100-year time horizons

Derek C. Manheim [a,b,*], Nazli Yeşiller [a], James L. Hanson [b], Donald R. Blake [c]

[a] Global Waste Research Institute, California Polytechnic State University, San Luis Obispo, CA, 93407, USA
[b] Civil and Environmental Engineering Department, California Polytechnic State University, San Luis Obispo, CA, 93407, USA
[c] Department of Chemistry, University of California-Irvine, Irvine, CA, 92697, USA

ARTICLE INFO

Keywords:
Landfill
Gas emissions
Methane
Landfill cover
Volatile organic compounds
Municipal solid waste
Climate impacts

ABSTRACT

Climate impacts of landfill gas emissions were investigated for 20- and 100-year time horizons to identify the effects of atmospheric lifetimes of short- and long-lived drivers. Direct and indirect climate impacts were determined for methane and 79 trace species. The impacts were quantified using global warming potential, GWP (direct and indirect); atmospheric degradation (direct); tropospheric ozone forming potential (indirect); secondary aerosol forming potential (indirect) and stratospheric ozone depleting potential (indirect). Effects of cover characteristics, landfill operational conditions, and season on emissions were assessed. Analysis was conducted at five operating municipal solid waste landfills in California, which collectively contained 13% of the waste in place in the state. Climate impacts were determined to be primarily due to direct emissions (99.5 to 115%) with indirect emissions contributing −15 to 0.5%. Methane emissions were 35 to 99% of the total emissions and the remainder mainly greenhouse gases (hydro)chlorofluorocarbons (up to 42% of total emissions) and nitrous oxide. Cover types affected emissions, where the highest emissions were generally from intermediate covers with the largest relative landfill surface areas. Landfill-specific direct emissions varied between 683 and 103,411 and between 381 and 37,925 Mg CO_2-eq./yr for 20- and 100-yr time horizons, respectively. Total emissions (direct + indirect) were 680 to 103,600 (20-yr) and were 374 to 38,108 (100-yr) Mg CO_2-eq./yr. Analysis time horizon significantly affected emissions. The 20-yr direct and total emissions were consistently higher than the 100-yr emissions by up to 2.5 times. Detailed analysis of time-dependent climate effects can inform strategies to mitigate climate change impacts of landfill gas emissions.

1. Introduction

Methane is the second most significant positive radiative climate driver (behind carbon dioxide) that adversely impacts earth's climate with atmospheric concentrations nearly monotonically increasing over the last several decades (IPCC, 2021). The main anthropogenic sources of methane in the atmosphere are oil and gas operations, agricultural activities, and municipal solid waste (MSW) landfills (USEPA, 2023).

Abbreviations: Alc, Alcohols; Alk, Alkanes; Alk/Alky, Aldehydes/Alkynes; Alke, Alkenes; Ar, Aromatic hydrocarbons; B, Baseline; Bsk, Arid, steppe, cold; CCL, Chiquita Canyon Landfill; Csa, Temperate, dry summer, warm summer; Csb, Temperate, dry summer, hot summer; D, Daily; D, Direct; *DGWP*, Direct global warming potential based on 20- or 100-yr values; $DGWR_1$, Primary direct emissions; $DGWR_2$, Secondary direct emissions; E_{LF}, Landfill emissions; F, Final; GCL, Geosynthetic clay liner; GHG, Greenhouse gas; GWP, Global warming potential; HH, Halogenated hydrocarbons; I, Indirect; I, Intermediate; *IGWP*, Indirect global warming potential impacts, Indirect global warming potential impacts; $IGWPO_3$, Indirect global warming potential of tropospheric ozone; $IGWP_{ODP}$, Indirect global warming potential for stratospheric ozone depleting potential; $IGWP_{SOA}$, Indirect global warming potential of tropospheric secondary organic aerosol; *IODP*, Indirect climate impacts from stratospheric ozone depletion; *IOFP*, Indirect climate impacts from tropospheric ozone formation potential; *ISOAP*, Indirect climate impacts from secondary organic aerosol formation potential; Ket, Ketones; L, Large size; M, Medium size; MIR, Maximum incremental reactivity; Mon, Monoterpenes; MSW, Municipal solid waste; *MW*, Molecular weight; NMVOC, Non-methane volatile organic compounds; *ODS*, Ozone depleting substance; *OFP*, (Tropospheric) Ozone formation potential; *ODP*, (Stratospheric) Ozone depletion potential; ON, Organic alkyl nitrates; PHL, Potrero Hills Landfill; RSC, Reduced sulfur compounds; SAL, Site A Landfill; SMRL, Santa Maria Regional Landfill; SOA, Secondary organic aerosol; *SOAP*, Tropospheric secondary organic aerosol formation potentials; TDL, Teapot Dome Landfill; WIP, Waste in place.

* Corresponding author at: Global Waste Research Institute, California Polytechnic State University, San Luis Obispo, California, 93407, USA.
E-mail address: dmanheim@calpoly.edu (D.C. Manheim).

https://doi.org/10.1016/j.wasman.2024.06.015
Received 19 October 2023; Received in revised form 17 May 2024; Accepted 18 June 2024
Available online 1 July 2024

While the relative contributions of fossil fuel operations have been decreasing, the contributions from animal farming and landfills have been increasing since the early 2000s (IPCC, 2021). Global landfill and waste methane emissions on the order of $1.90x10^9$ Mg CO_2-eq./yr were reported for 2017 constituting 18% of total anthropogenic and 9% of total methane emissions (Saunois et al., 2020). California landfill methane emissions of $8.5x10^6$ Mg CO_2-eq./yr constitute approximately 2% of the state GHG emissions (CARB, 2020).

Temporal gas generation trends in landfills closely follow waste temperature and moisture content trends that are directly influenced by local climate. High gas generation occurs at relatively high waste temperatures and high waste moisture contents, low gas generation is associated with low temperatures and low moisture contents (particularly in arid climates), and arrested gas generation is observed at below freezing conditions (Hanson et al., 2005, Hanson et al., 2006). Enhanced waste decomposition is projected at landfills due to increasing air temperatures resulting in higher methane releases into the atmosphere providing a positive climate feedback (IPCC, 2021). Population and consumption per capita are projected to increase in both developed and developing countries resulting in increases in waste generation and landfill disposal as landfilling continues to be the main means of solid waste management in many parts of the world (Kaza et al., 2018). These factors collectively are expected to stress MSW management infrastructure and intensify climate impacts of landfills.

Methane has direct effects on the atmosphere and as a main landfill gas constituent (45–60 %v/v) (Tchobanoglous et al., 1993) typically is the only gas considered in the assessment of the climate change impacts of municipal solid waste landfills (Mønster et al., 2019, IPCC, 2021). However, trace greenhouse gas (GHG) constituents present in landfill gas including nitrous oxide and chlorinated and fluorinated species, (hydro)chlorofluorocarbons (termed F-gases herein) also have direct climate impacts (IPCC, 2021). In addition, chlorofluorocarbons (CFCs) and hydrochlorofluorocarbons (HCFCs) are stratospheric ozone depleting substances (ODSs) (WMO, 2018). Furthermore, landfill gas contains many additional trace non-methane volatile organic compounds (NMVOCs) that produce climate impacts. Atmospheric degradation of NMVOCs leads to the production of CO_2, which is a known secondary direct effect on climate change (Boucher et al., 2009). The NMVOCs participate in numerous photochemical reactions in the troposphere considered to be critical precursors of ozone, photochemical smog, and secondary organic aerosols (Atkinson and Arey, 2003). NMVOCs, through complex photochemical reactions, indirectly affect global climate change by reducing the efficiency of GHG oxidation and thus promote accumulation of GHGs in the atmosphere (Collins et al., 2002). Fugitive emissions of all of these gases (main and trace) are relevant and of concern in evaluation of impacts of landfills on the earth-atmosphere system.

Even though a large number of studies has been conducted on landfill methane emissions, limited information is available on emissions of trace gases from landfill facilities and associated climate impacts. A recent comprehensive review of worldwide landfill gas emissions data identified methane, nitrous oxide, and NMVOC fluxes to be $-4.5x10^1$ to $4.15x10^4$, $-2.5x10^{-3}$ to $3.75x10^1$, and $-2x10^{-3}$ to $7.32x10^{-1}$ g/m^2-day, respectively, where positive values correspond to emissions from the landfill to the atmosphere and negative values correspond to uptake of chemicals from the atmosphere into the landfill (Manheim et al., 2021a). In a previous study, the authors demonstrated that F-gases emitted from landfills exert disproportionate direct climate impacts due to their high global warming potentials (GWPs) (Yeşiller et al., 2018). For CO_2-eq. emissions at California landfills, the relative contributions of F-gases to total emissions (summation of methane and F-gas emissions in the study) were determined to range from 1 to 68% in the dry season (Yeşiller et al., 2019) and F-gas contributions to total emissions (summation of methane, F-gas, and nitrous oxide emissions in the study) were determined to range from 1 to 99% for annual analysis (Manheim et al., 2021b). Correlations between geotechnical cover characteristics and climate-forcing GHG and NMVOC emissions have been reported by Hanson et al., (2023a,b) with a focus on soil covers.

The main objective of this investigation was to provide a comprehensive and systematic analysis of surface emissions and associated time-dependent climate forcing impacts from California landfills representative of both the main landfill gas methane and trace NMVOCs. Analysis was conducted using 20- and 100-yr time horizons to evaluate climate impacts of both short- and long-lived landfill gases. Field campaigns were conducted to determine surface fluxes of 80 individual gases at five landfills over the two main seasons, wet and dry, in California. Analysis was conducted for all three cover categories: daily, intermediate, and final, used at active landfills. Both the magnitude and relative contributions of the main and trace gas emissions and the direct and indirect emissions to total climate impacts were assessed. Investigation of a wide variety of gases and landfill operational conditions, as well as multiple environmental conditions, climatic forcings, and time horizons allow for comprehensive understanding of the atmospheric impacts of MSW landfills. Results from the analysis presented herein provide quantitative insight as to the effectiveness of current (i.e., short-term) and viability of proposed (i.e., long-term) strategies to mitigate climate impacts of MSW landfills.

2. Experimental investigation

2.1. Field testing program

Field campaigns were conducted at five municipal solid waste landfills (Table 1). Santa Maria Regional Landfill (SMRL) and Teapot Dome Landfill (TDL) are medium-size facilities with waste in place (WIP) between 4,000,000 and 40,000,000 m^3. Potrero Hills Landfill (PHL), Site A Landfill (SAL), and Chiquita Canyon Landfill (CCL) are large-size facilities with waste in place greater than 40,000,000 m^3. The five sites collectively contained 13% of the waste in place in active California landfills. The landfills are located in three climate zones: Csb (temperate, dry summer, hot summer), Csa (temperate, dry summer, warm summer), and Bsk (arid, steppe, cold) (Köppen-Geiger analysis, Beck et al., 2018). Tests were conducted over the two main seasons in California: wet (winter) and dry (summer). The cover categories investigated were daily, intermediate, and final. The daily covers included clean and contaminated soils and alternative daily covers (auto shredder residue, green waste, wood waste, and construction and demolition waste). Intermediate covers included soil, soil-concrete fines mix, and soil overlain by old or fresh green waste. The final covers included conventional compacted clayey covers, a composite GCL-compacted clay liner, and an alternative evapotranspirative cover. At a given landfill, 4 to 7 cover types were tested for a total of 29 individual covers investigated in the study. Test locations were selected randomly. All of the landfills had operational gas collection and removal systems in place at the time of testing.

Field testing included determination of surface fluxes of 80 landfill gas constituents: three anthropogenic GHGs (methane, nitrous oxide, and NMVOC (hydro)chlorofluorocarbons (F-gases, 13 species)), and 65 additional trace NMVOCs. The 65 additional trace NMVOCs were grouped under 10 chemical families: reduced sulfur compounds (RSC), halogenated hydrocarbons (HH), organic alkyl nitrates (ON), alkanes (Alk), alkenes (Alke), Aldehydes/Alkynes (Ald/Alky), aromatic hydrocarbons (Ar), monoterpenes (Mon), alcohols (Alc), and ketones (Ket). Among these chemicals, flux and emissions analyses are provided herein for 5 species, HFC-365mfc (GHG) and n-undecane, n-propyl-benzene, 2-butanol, and butanone, for the first time from non-soil daily covers in landfill systems. In addition, this work represents the first systematic comparison of 20-yr versus 100-yr (GWP time horizons) climate impacts of landfills. Details for the 80 gases included in the investigation are provided in Table A1.

Table 1
Landfill Characteristics.

Landfill	Size[a]	Area (ha)	WIP[b] (m^3)	Permitted Disposal (tons/day)	Avg. Daily Temp. (°C)	Annual Ppt. (mm)	Climate Zone	Cover Fraction[c] (%)		
								D	I	F
Santa Maria Regional Landfill (SMRL)	M	100	1,360,577	858	14.9	462	Csb	0.1	69.3	30.6
Teapot Dome Landfill (TDL)	M	29	3,038,622	800	17.4	278	BSk	15.5	84.5	0
Potrero Hills Landfill (PHL)	L	139	52,928,614	4,330	16.1	630	Csa	3.0	91.0	6.0
Site A Landfill (SAL)	L	191	44,173,397	11,150	15.8	387	Csb	0.6	89.5	9.9
Chiquita Canyon Landfill (CCL)	L	104	55,227,178	6,000	18.2	462	Csb	8.3	63.8	27.8

[a] M = medium, L = large;
[b] Obtained from SWIS (Solid Waste Information System);
[c] D = Daily, I = Intermediate, F = Final.

2.2. Determination of flux and emissions

The tests and analysis were conducted using the same equipment and methodology as in prior investigations (Yeşiller et al., 2018, Hanson et al., 2023a,2023b). Surface fluxes of all gases were measured using custom-built large-scale stainless-steel static flux chambers with dimensions of 1 m length x 1 m width x 0.4 m height, where data were collected from two chambers representing a small area of the cover at each test location. A total of five gas samples over time were obtained per chamber using 60- and 120-minute testing periods. The gas samples were collected using custom-built, 2-L capacity stainless steel evacuated canisters and analyzed using two integrated VOC analytical systems with methane, nitrous oxide, and NMVOC detection limits of 100 ppbv, 50 ppbv, and 0.05–50 pptv, respectively. Flux was determined for each chamber as the product of the concentration gradient (i.e., change in concentration with time, dC/dt) and the volume:area ratio of the chamber (Rolston et al., 1986). The change in concentration with time was fit with a linear regression relationship with a target threshold coefficient of determination value of $R^2 \geq 0.90$. At each measurement location, two chambers were deployed, one chamber with the 60-minute testing time and one chamber with the 120-minute testing time. Overall, nearly 65,000 individual gas concentration measurements were made to determine the gas fluxes at the landfills included in the investigation. Fluxes were scaled up to cover-specific and sitewide emissions using the relative areas of the different cover categories and the total area of a given landfill (Table 1).

In addition to flux and emissions, analysis was conducted to determine specific gas concentrations for the species included in the test program. Raw gas concentrations were determined by sampling from entry points to the gas-to-energy plants or flares at the landfills using the 2-L capacity stainless steel evacuated canisters. Ambient gas concentrations were obtained using the data from the first (time zero) canister samples in the flux chamber tests, which represent conditions near the ground surface. Background air concentration data, available for 6 chemical families, were obtained from Advanced Global Atmospheric Gases (AGAGE) and USEPA AirData measurement programs (Prinn et al., 2018, USEPA, 2022).

2.3. Climate Change: Direct and indirect impacts analyses

The classifications used for reporting emissions were baseline (Mg/yr), direct (Mg CO_2-eq./yr), and indirect (Mg CO_2-eq./yr). Baseline emissions represented the total mass per time of gas species emitted from the site without scaling using GWPs. The baseline emissions calculated for individual gases were used to determine the direct and indirect climate impacts. The analysis was conducted using the same approach as in a prior investigation (Hanson et al. 2023a). A summary is provided herein. CO_2-eq. emissions were determined using 20- and 100-yr data (Table A1) to assess short- and long-term climate impacts.

The total direct emissions for each landfill were calculated by summing the primary ($DGWR_1$) and secondary ($DGWR_2$) direct emissions (Equations (1) and (2)). Primary direct emissions analysis was conducted for anthropogenic GHGs, methane, nitrous oxide, and F-gases (13 species) and also for 15 additional NMVOCs. Direct climate forcing ($DGWR_1$, Mg CO_2-eq./yr) was estimated using Equation (1), where $E_{LF,i}$ is the chemical-specific landfill emissions and $DGWP_i$ is the chemical-specific direct GWP based on 20- or 100-yr values (IPCC, 2021). Direct impact analysis also included secondary production of carbon dioxide from atmospheric degradation of all 80 landfill gas species investigated. $DGWR_2$, (Mg CO_2-eq./yr) was estimated using Equation (2), where MW_i is the chemical-specific molecular weight and $N_{c,i}$ is the total number of carbon atoms (Majumdar and Srivastava, 2012).

$$DGWR_1 = \sum_{i=1}^{30}[E_{LF,i} \times DGWP_i] \quad (1)$$

$$DGWR_2 = \sum_{i=1}^{80}[\frac{E_{LF,i}}{MW_i} \times N_{c,i}*44] \quad (2)$$

Indirect global warming potential impacts ($IGWR$, Mg CO_2-eq./yr) for the 65 additional NMVOCs were calculated using Equation (3), where $IGWP_i$ is the chemical-specific indirect GWP. Indirect 20- and 100-yr GWP values were available for 15 NMVOCs (Johnson and Derwent, 1996, Collins et al., 2002, Hodnebrog et al., 2018). For the remaining 50 NMVOCs, the $IGWP_i$ were estimated by using scattered, 3-D interpolation through application of the natural neighbor method (MATLAB, 2022). Experimental reaction rate coefficients of each NMVOC with hydroxyl, chlorine, and nitrate radicals were used as predictor variables (McGillen et al., 2020). The indirect climate impacts from ozone formation potential ($IOFP$, Mg CO_2-eq./yr) were calculated using Equation (4), where OFP_i (g O_3/g NMVOC) is the chemical-specific ozone formation potential based on maximum incremental reactivity (MIR) and $IGWPO_3$ is the indirect GWP of tropospheric ozone (Wuebbles et al., 1994). Chemical-specific tropospheric ozone formation potentials (OFP_i) for methane and 52 NMVOCs were quantified using the MIR scale (Carter, 2010). The indirect climate impacts from secondary organic aerosol formation potential ($ISOAP$, Mg CO_2-eq./yr) were calculated using Equation (5), where $SOAP_i$ (g SOAP/g NMVOC) is the chemical-specific tropospheric secondary organic aerosol (SOA) formation potential and $IGWP_{SOA}$ is the indirect GWP of tropospheric SOA (Unger, 2014). Chemical-specific tropospheric SOA formation potentials ($SOAP_i$) were determined using available fractional aerosol coefficients

for 18 gases (Grosjean and Seinfeld, 1989). The indirect climate forcings for ODSs (*IODP*) were calculated using Equation (6), where $IGWP_{ODP,i}$ is the chemical-specific indirect GWP for stratospheric ozone depleting potential available for 12 gases (WMO, 2018, IPCC, 2021). The indirect emissions (Mg CO_2-eq./yr) for each landfill were calculated by summing the *IGWR*, *IOFP*, *ISOAP*, and *IODP* values obtained from Equations 3–6.

$$IGWR = \sum_{i=1}^{65}[E_{LF,i} * IGWP_i] \tag{3}$$

$$IOFP = IGWP_{O_3} * \sum_{i=1}^{53}[E_{LF,i} * OFP_i]. \tag{4}$$

$$ISOAP = IGWP_{SOA} * \sum_{i=1}^{18}[E_{LF,i} * SOAP_i] \tag{5}$$

$$IODP = \sum_{i=1}^{12}[E_{LF,i} * IGWP_{ODP,i}] \tag{6}$$

3. Results

3.1. Gas concentration and flux

Concentration data are presented for the main GHGs and the 10 NMVOC families included in the investigation in Fig. 1a. The 13 F-gases are included under main GHGs and thus the NMVOC designation is used

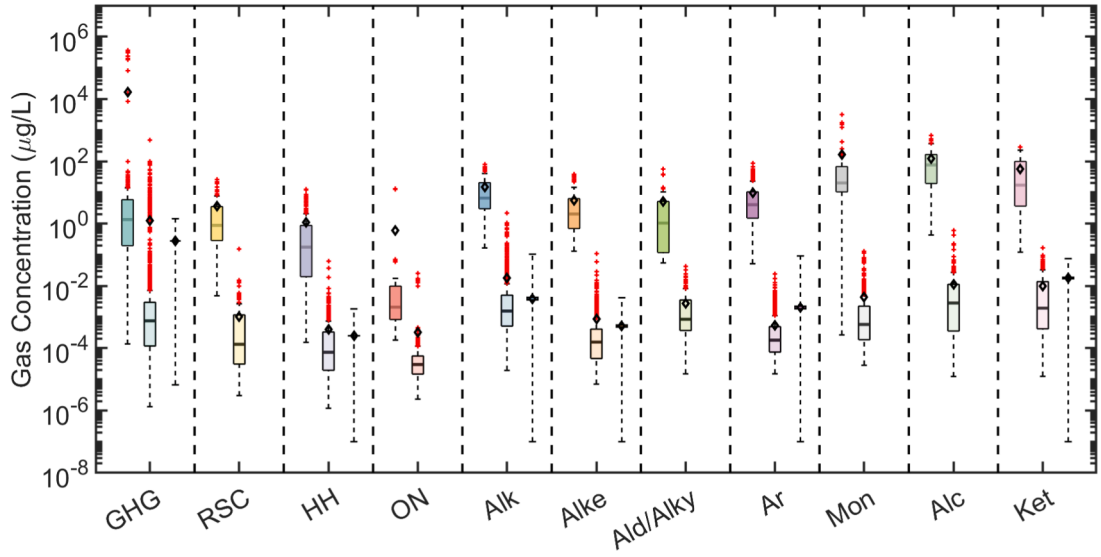

(a) Measured Concentrations (landfill gas, ambient, available background data presented left to right for each chemical family)

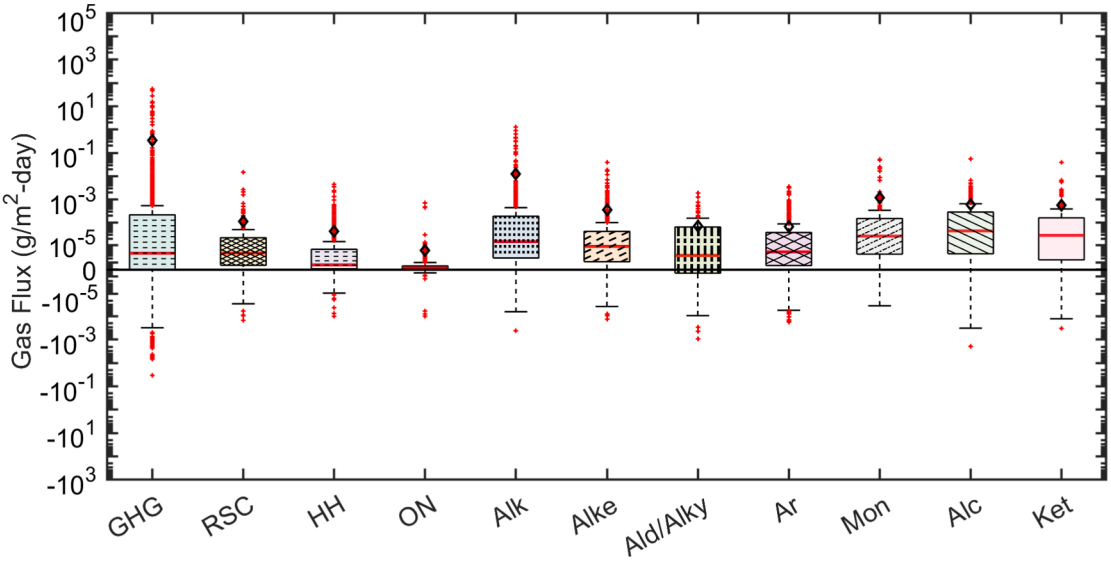

(b) Measured Fluxes

Fig. 1. Gas Concentration and Flux by Chemical Family.

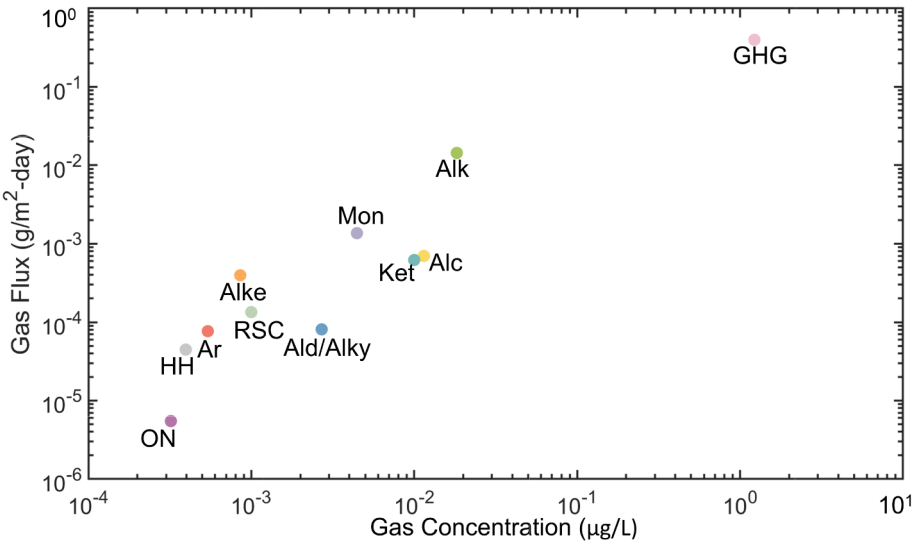

(c) Variation of Flux with Concentration

Fig. 1. (*continued*).

for the remaining 65 NMVOC gases in the following sections. Raw gas data, gas concentrations, and available background air concentration data are presented in Fig. 1a. The box, horizontal line within each box, diamond, and red datapoints in each dataset of Fig. 1a and 1b represent the interquartile range, median, mean, and outlying data, respectively. The raw, ambient, and background concentrations varied between $1.36x10^{-4}$ to $3.67x10^{5}$, $1.33x10^{-6}$ to $4.84x10^{2}$, and $6.65x10^{-6}$ to $1.43x10^{0}$ µg/L, respectively for the main GHGs. The raw, ambient, and background concentrations varied between $4.80x10^{-3}$ to $2.62x10^{1}$, $3.01x10^{-6}$ to $1.53x10^{-1}$, and $1.0x10^{-7}$ to $1.04x10^{-1}$ µg/L, respectively for the NMVOCs.

Gas fluxes determined in the study are presented in Fig. 1b. Both positive (releases to the atmosphere) and negative (uptake from the atmosphere) surface fluxes were measured. A virtual zero position is used in the logarithmic scale plots to enable presenting positive and negative data. Data are presented for the GHGs and the 10 NMVOC families. Overall, methane, nitrous oxide, F-gas, and NMVOC fluxes measured in the study ranged from $-3.37x10^{-2}$ to $5.49x10^{1}$, $-1.97x10^{-3}$ to $1.15x10^{-1}$, $-9.13x10^{-4}$ to $2.27x10^{-1}$, and $-1.93x10^{-3}$ to $1.28x10^{0}$ g/m^2-day, respectively. Variation of average fluxes with average ambient concentrations obtained in the investigation are presented in Fig. 1c.

Flux data are summarized by landfill, cover category, and season for the GHGs (methane, nitrous oxide, and 13 F-gases) and the NMVOCs in Fig. 2. Landfill-specific mean GHG and NMVOC fluxes ranged from $6.73x10^{-2}$ to $7.76x10^{-1}$ and $2.56x10^{-5}$ to $6.60x10^{-3}$ g/m^2-day, respectively. Cover-specific mean GHG and NMVOC fluxes ranged from $2.40x10^{-3}$ to $7.50x10^{-1}$ and $3.35x10^{-5}$ to $7.30x10^{-3}$ g/m^2-day, respectively. Seasonal mean GHG and NMVOC fluxes were $2.46x10^{-1}$ to $4.51x10^{-1}$ and $1.80x10^{-3}$ to $1.90x10^{-3}$ g/m^2-day, respectively. At a given landfill, variation of positive GHG and NMVOC fluxes were up to 4 to 8 and 4 to 6 orders of magnitude, respectively. At a given landfill, variation of positive GHG fluxes for daily, intermediate, and final covers were up to 2 to 4, 1 to 5, and 1 to 2 orders of magnitude, respectively. At a given landfill, variation of positive NMVOC fluxes for daily, intermediate, and final covers were up to 3 to 4, 3 to 5, and 2 to 4 orders of magnitude, respectively. Seasonal GHG and NMVOC variations were less than one order of magnitude.

3.2. Gas emissions

Baseline, direct, and indirect emissions by landfill and chemical family for 100-yr GWP analyses are presented in Fig. 3. Arithmetic-scaled fractional contributions are superimposed over the logarithmic scaling in Figs. 3-6. The baseline, direct, and indirect GHG emissions were 4.97 to 1,221 Mg/yr, 379 to 37,918 Mg CO_2-eq./yr, and −4,625 to 140 Mg CO_2-eq./yr, respectively. The baseline, direct, and indirect NMVOC emissions were 0.741 to 46.5 Mg/yr, 1.92 to 146 Mg CO_2-eq./yr, and 9.78 to 858 Mg CO_2-eq./yr, respectively. At a given landfill, variation of positive baseline and direct GHG emissions were 3 to 4 and 2 to 3 orders of magnitude, respectively.

Baseline and direct CO_2-eq. emissions by landfill and cover category for 20- and 100-yr GWP analyses are presented in Fig. 4. The baseline emissions for the landfills in the study ranged from 5.71 Mg/yr (SMRL) to 1,223 Mg/yr (TDL). The 20-yr and 100-yr direct emissions for the landfills included in the study were: 683 and 381 Mg CO_2-eq./yr (SMRL); 103,411 and 37,925 Mg CO_2-eq./yr (TDL); 94,114 and 34,602 Mg CO_2-eq./yr (PHL); 87,524 and 32,565 Mg CO_2-eq./yr (SAL); and 64,715 and 28,608 Mg CO_2-eq./yr (CCL), respectively. Indirect emissions are also presented in Fig. 4. The 20-yr and 100-yr indirect emissions for SMRL, TDL, PHL, SAL, and CCL were −2.57 and −6.40, 189 and 183, −142 and −9.66, −85.7 and −40.9, and −3,337 and −3,768 Mg CO_2-eq./yr, respectively. Of the cover categories investigated, intermediate cover baseline and direct emissions contributed most to the total emissions observed across all sites. An exception to this trend was observed for CCL, where daily cover baseline and direct emissions were highest of the cover categories investigated. Large negative daily cover indirect emissions contributions were observed both at CCL and PHL.

Direct and indirect emissions for each landfill as a function of climate impact category for both GWP time horizons are presented in Fig. 5. Direct emissions varied between 683 and 103,411 and between 381 and 37,925 Mg CO_2-eq./yr for 20- and 100-yr time horizons, respectively. Indirect emissions varied between −3,337 and 189 and between −3,767 and 183 Mg CO_2-eq./yr for 20- and 100-yr time horizons, respectively. Total emissions are presented in Fig. 6 and varied between 680 and 103,600 (20-yr analysis) and between 374 and 38,108 (100-yr analysis) Mg CO_2-eq./yr. Total emissions by cover category for the 20-yr time horizon were 150 to 51,000; 420 to 99,000; and 26 to 3,200 Mg CO_2-eq./yr for daily, intermediate, and final covers, respectively. Total

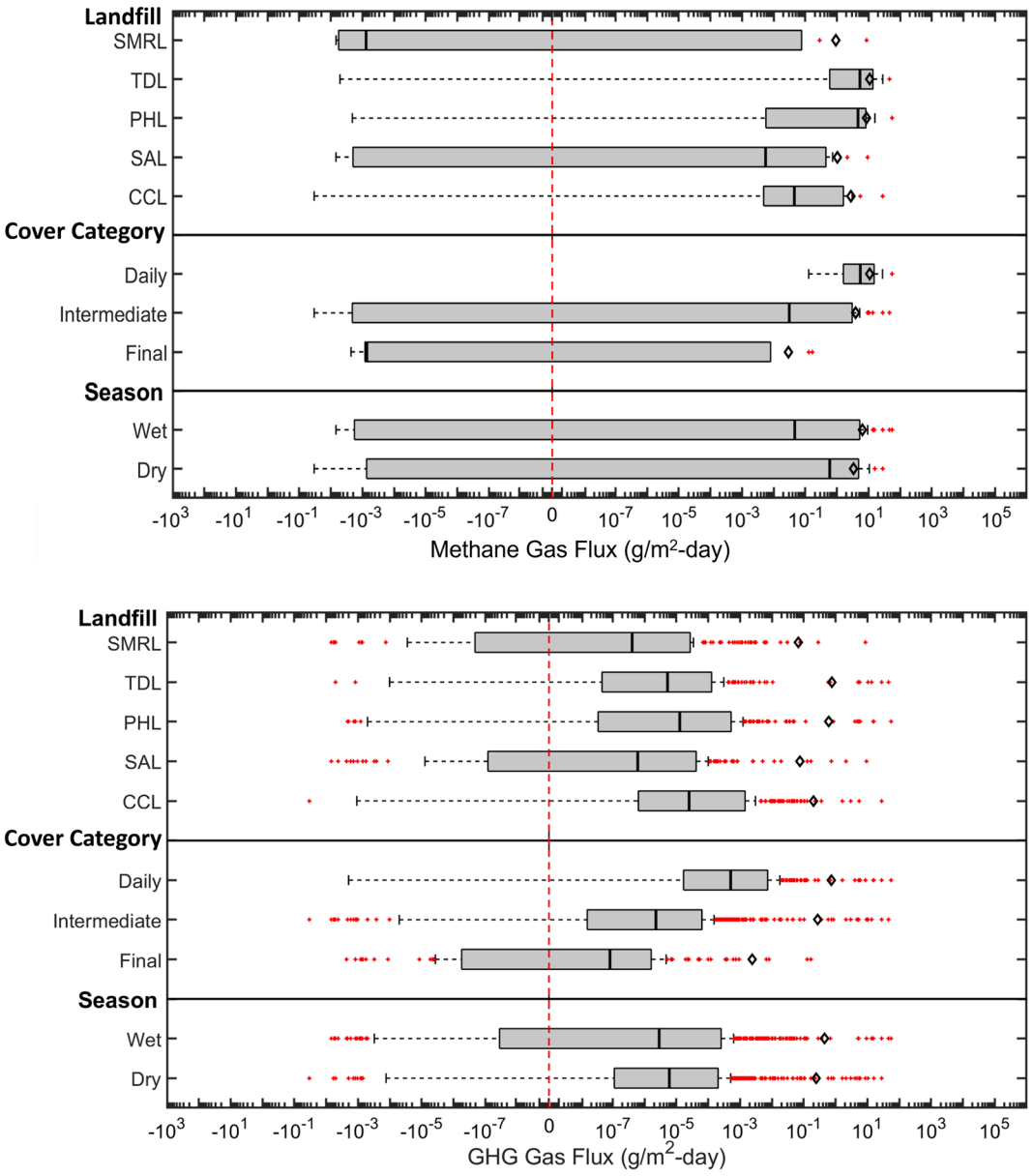

Fig. 2. Summary of Fluxes Measured in the Investigation.

emissions by cover category for the 100-yr time horizon were 55 to 20,273; 198 to 36,536; and 21 to 1,161 Mg CO_2-eq./yr for daily, intermediate, and final covers, respectively. Ratios of 100-yr to 20-yr gas emissions varied between 0.069 and 2.49 and are presented in Fig. 7.

4. Discussion

Raw landfill gas concentrations of the chemicals included in the study were consistently higher than the ambient and background concentrations (Fig. 1a). The mean ambient concentrations were generally higher than the mean background air concentrations by 1 order of magnitude with the exception of aromatic hydrocarbons and ketones (background concentrations slightly higher than ambient concentrations). The differences between the ambient and background air concentrations were higher for the anthropogenic GHGs than the NMVOCs. Within the GHGs, the difference between ambient and background concentrations were higher for methane than for nitrous oxide and F-gases (Hanson et al., 2020). Gas fluxes were directly correlated to ambient near ground surface concentrations, supporting the need for regular surface gas monitoring at landfills (Fig. 1c).

Positive fluxes were measured for all 80 gases from all three cover categories at all landfills included in the investigation. Overall, four types of flux data were obtained: positive flux, negative flux, below detection limit data, and below regression limit data, where the majority of the data consisted of positive fluxes. F-gas and NMVOC fluxes were statistically skewed to more positive values than methane and nitrous oxide fluxes.

Highest fluxes were obtained for GHGs, alkanes, monoterpenes, alcohols, and ketones (Fig. 1b). Methane flux was higher than the fluxes of the other GHGs and the remaining NMVOCs (Fig. 2). Overall, variability of flux was lower for the NMVOCs (all trace constituents) than the GHGs, which included both main (methane) and trace gases (nitrous oxide and F-gases) (Figs. 1 and 2). Methane flux is affected by both waste and cover processes. Waste characteristics and landfill operational conditions each influence methane loading underlying the various covers (Tchobanoglous et al., 1993). In addition, methane undergoes transformation in

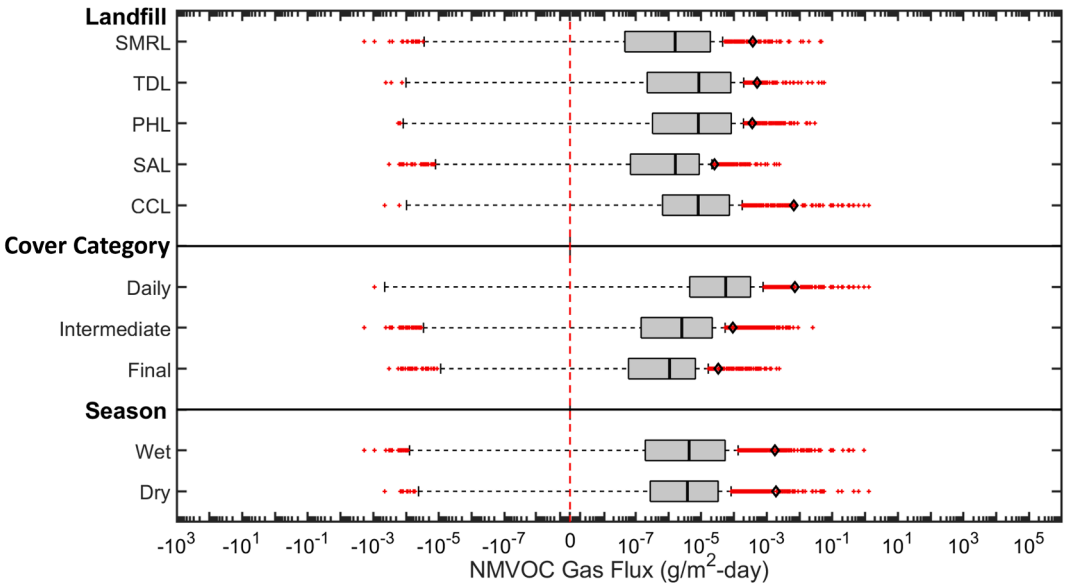

Fig. 2. (*continued*).

cover materials mainly through biological oxidation (e.g., Chanton et al., 2011). Furthermore, methane flux is affected by cover geotechnical properties (Hanson et al., 2023a). Coupled effects of the spatio-temporal variations in waste methane generation, cover methane oxidation processes, and cover engineering properties likely contributed to the high variations of methane fluxes. F-gas and NMVOC fluxes are generated through direct volatilization from waste materials in addition to biogenic generation during various stages of waste decomposition (Christensen et al., 1996). Studies on biological transformation processes for F-gases and select NMVOC chemical families (e.g., aromatics, halogenated hydrocarbons) in soil covers indicate generally low to moderate reactivity (e.g., Scheutz and Kjeldsen, 2003), which along with low mobility in the waste mass due to phase partitioning and adsorptive processes (Manheim et al., 2021a) may have contributed to the relatively low variation in NMVOC fluxes.

Flux varied mainly by cover category decreasing from daily to intermediate to final covers, by landfill, and also to a lesser extent by season. Median flux decreased by 4 and 2 orders of magnitude from daily to final covers for GHGs and NMVOCs, respectively (Fig. 2). From daily, to intermediate, to final covers, the cover materials transition from generally coarse-grained, relatively loosely placed, low thickness, cohesionless, and low solids content, to fine-grained, well-compacted, high thickness, cohesive, and high solids content materials. The combined effect of the transition to final cover results in increased resistance to gas transfer. In addition, the coarse-grained covers have well-connected pores that readily transmit fluids, whereas fine-grained covers have occluded pores that resist flow of fluids (Yeşiller et al., 2018). Seasonal effects were minimal as the climate zones with landfills in California vary over a relatively narrow range with comparatively low variations in average daily temperature and annual precipitation (Table 1). Flux was not directly correlated to the size of the landfills, where maximum inter-landfill variations in median GHG and NMVOC fluxes was less than 2 and 1 orders of magnitude, respectively. The relatively comparable fluxes at the mid-sized landfills (SMRL and TDL) to the large landfills (PHL, SAL, and CCL) were attributed to presence of low amount of fine-grained soils and plastic fines and prevalence of sandy soils and silts with low plasticity in the cover soils at the smaller Santa Maria Regional Landfill and Teapot Dome Landfill (Hanson et al., 2023a). In addition, no final covers were present at TDL at the time of the investigation.

The direct emissions were essentially positive and high, whereas indirect emissions were mostly negative and low (Figs. 3-5). Baseline and direct emissions at the study landfills were dominated by GHG emissions (Fig. 3). Within the GHGs, the main landfill gas methane generally contributed most to both baseline and direct emissions (Fig. 3). However, the relative contributions of methane decreased from baseline to direct emissions analysis and relative contributions of the trace GHGs nitrous oxide, and, in particular F-gases, significantly increased due to the comparatively high global warming potentials, particularly of the F-gases. For 20-yr analysis, the GWP for nitrous oxide was 273 and the GWPs for the F-gases varied from 575 to 12,400 and for 100-yr analysis, the GWP for nitrous oxide was 273 and the GWPs for the F-gases varied from 160 to 11,200 (Table A1).

Emission fractions were determined by taking the quotient of the baseline, direct (20-yr/100-yr GWP), or indirect (20-yr/100-yr GWP) emissions and the total emissions (either baseline or 20-yr/100-yr GWP). Direct and indirect emission fraction calculations represented the relative contributions of either positive or negative emissions along with positive or negative GWP weighting. Across all landfills, calculated direct emissions were mainly positive, ranging from 99.5 to 115% of the total emissions. The direct emission fractions were either near or above 100% due to the high mainly positive surface emissions and the high positive radiative forcing associated with the main GHGs and select NMVOCs. Calculated indirect emissions were generally negative, ranging from −15 to 0.5% of the total emissions. The indirect emissions (and associated emission fractions) were lower than the direct emissions due to the relatively higher direct GWP of the gases compared to the parameters describing indirect emissions (Equations 3–6).

Emission fractions were also determined on a chemical family basis by taking the quotient of family-specific baseline or combined direct and indirect (20-yr/100-yr GWP) emissions and the total emissions (either baseline or 20-yr/100-yr GWP) from each landfill. For methane, baseline, 20-yr GWP direct, and 100-yr GWP direct emissions were 75 to > 99%, 53 to 99%, and 35 to 99% of the total emissions, respectively. For F-gases, baseline, 20-yr GWP direct, and 100-yr GWP direct emissions were 0.02 to 1.9%, 0.8 to 42%, and 0.8 to 42% of the total emissions, respectively. Direct GWPs were typically highest for the CFCs followed by the HCFCs, and HFCs, then nitrous oxide, and methane (Table A1). The high direct emissions resulted from the high positive radiative forcing of these gases. The contributions of secondary carbon dioxide formation to direct emissions were relatively low (Fig. 5). Positive indirect emissions were mainly associated with the alkane, alkene, aldehyde/alkyne, aromatic, and alcohol chemical families. Negative indirect emissions were generally associated with the GHGs (mainly F-gases) and

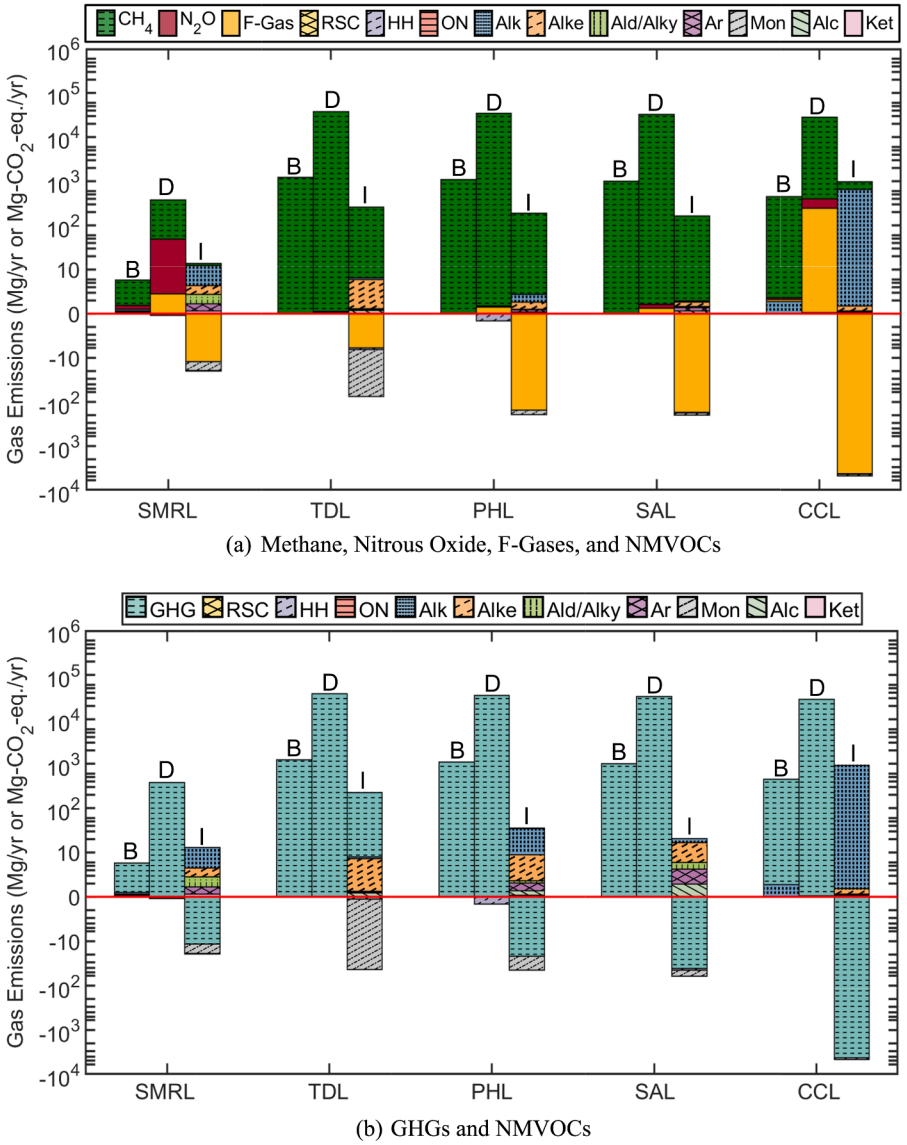

Fig. 3. Baseline (B), Direct (D), and Indirect (I) Gas Emissions by Landfill and Chemical Family.

monoterpenes (Fig. 3). In general, indirect emissions were dominated by the stratospheric ozone depleting potential and the secondary organic formation potential, where contributions from the indirect global warming potentials and tropospheric ozone formation were not as significant (Fig. 5). Overall, positive and negative emissions were mainly dominated by direct climate forcing and indirect stratospheric ozone depletion contributions, respectively.

The largest contributions to total emissions were generally from the intermediate covers (Figs. 4 and 6). These covers had the highest relative surface areas at the study landfills (Table 1) and moderate fluxes (Fig. 2). The relatively low intermediate cover emissions at CCL were largely attributed to the operational practice of placement of a layer of green waste over intermediate soil covers for erosion control on perimeter slopes. The green waste layer likely promoted methane oxidation (Barlaz et al., 2004, Abichou et al., 2006), and as methane was the predominant constituent of baseline and direct emissions categories low methane emissions resulted in reduced overall emissions from these covers. Even though the fluxes from daily covers were high, the contributions of these to the total whole-site emissions were generally low (<16%) due to the relatively low areas at the landfills. Relative contributions of final covers were 0 to 32% (Fig. 6).

The analysis time horizon affected the climate forcing emissions. The 20-yr GWP emissions data were consistently higher than the 100-yr GWP data for direct, indirect, and total climate-forcing emissions (Figs. 4-7). Ratios of 100-yr to 20-yr gas emissions were lower than 1 (essentially lower than 0.5) for direct and total gas emission scenarios (Fig. 7). The differences between 20-yr and 100-yr analysis were lower for indirect emissions than direct emissions (Fig. 5). The direct 20-yr GWPs were higher than direct 100-yr GWPs, the indirect 20-yr GWPs were higher than indirect 100-yr GWPs, and stratospheric ozone depletion GWPs ($IGWP_{ODP}$) were relatively similar between the two time horizons. Indirect emissions for SMRL and CCL from 20-yr analysis was lower than the 100-yr analysis. The differences mainly resulted from the higher emissions of NMVOCs relative to GHGs from these two sites (in particular from daily covers), which included high ODP and SOAP gases.

The combined total emissions from the 5 study landfills were 347,070 and 130,440 Mg CO_2-eq./yr for 20-yr and 100-yr time horizons, respectively. The combined methane emissions were 311,485 and 114,400 Mg CO_2-eq./yr for 20-yr and 100-yr time horizons, respectively representing 3.7 and 1.3% of estimated California landfill methane emissions of 8.5×10^6 Mg CO_2-eq./yr based on inventory analysis provided in CARB (2020). The total waste mass at the 5 landfills was 13% of the waste in place in California, higher than the relative emissions contributions from these landfills to state totals. Inclusion of the indirect

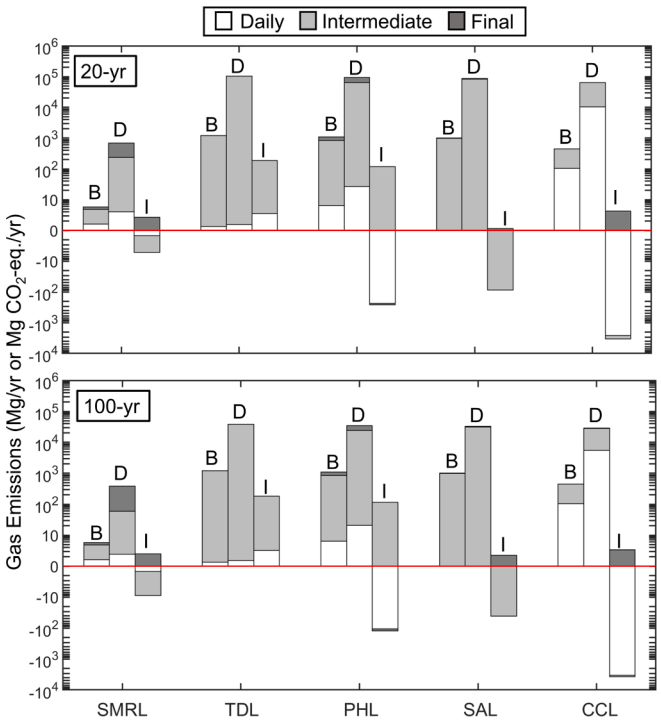

Fig. 4. Baseline (B), Direct (D), and Indirect (I) Gas Emissions by Landfill and Cover Category for 20-yr and 100-yr Analyses.

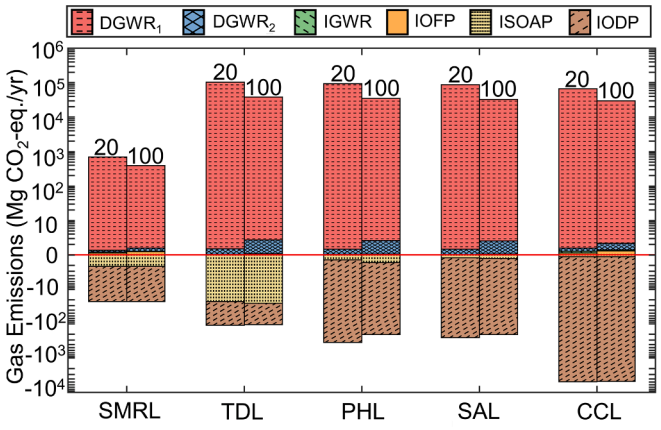

Fig. 5. Total Direct and Indirect Emissions by Climate Impact Category.

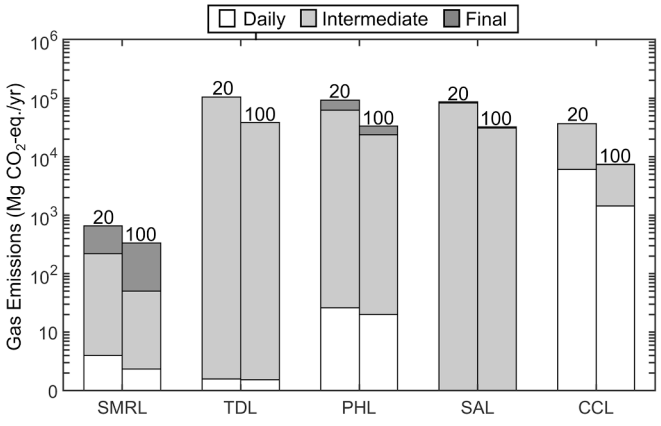

Fig. 6. Total Gas Emissions.

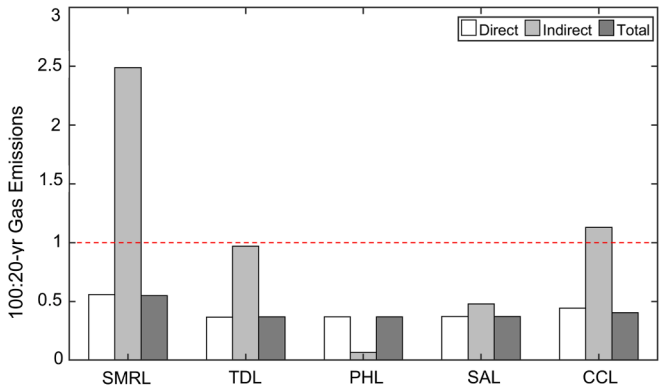

Fig. 7. Ratios of 100-yr to 20-yr Direct, Indirect, and Total Gas Emissions.

effects in the total emissions calculations offset total climate forcing impacts for each landfill, reducing the total emissions by 0.03 to 15%. Indirect emissions were relatively low for GHGs and higher for NMVOCs and affected total emissions for NMVOCs more than GHGs. The effects of indirect emissions were most significant for NMVOCs and 100-yr GWP analysis.

Parametric analyses were conducted by changing the areal extent of the different covers to further study the effects of cover categories on emissions. First, the areal extents of intermediate covers were reduced by 50% (converting this area to final cover) without changing the areas of daily covers. This analysis resulted in decreases in total emissions at the study landfills. For 20-yr GWP analysis, the decreases in total emissions were 12% for SMRL, 48% for TDL, 37% for PHL, 48% for SAL, and 9% for CCL. For 100-yr GWP analysis, the decreases were 48% for TDL, 37% for PHL, 48% for SAL, and9 % for CCL, respectively. At SMRL, total emissions increased (for the 100-yr GWP analysis) by 10% mainly due to an increase in final cover associated emissions of nitrous oxide. Moderate to high positive fluxes of nitrous oxide were observed at this final cover location. Due to potential generation of nitrous oxide in soil covers associated with biological N cycling (i.e., nitrification/denitrification), there is uncertainty as to whether the elevated nitrous oxide emissions from SMRL can be attributed to cover- or waste-specific generation mechanisms. This particular landfill is located in an agriculturally intensive region, likely receiving a waste composition that is highly organic and elevated in macronutrients (N, P), which may have contributed to the high nitrous oxide emissions observed in final cover areas.

Second, the areal extents of daily covers were set to 1% representative of working face and immediate surrounding areas. The daily cover areas in excess of 1% were converted to intermediate cover areas. This analysis was conducted for TDL, PHL, and CCL with daily cover areas larger than 1% of the total landfill surface area (Table 1). Conversion of daily cover areas to intermediate cover areas resulted in significant reductions in total emissions. For the three sites, TDL, PHL and CCL, total emissions decreased by 67, 49 and 80%, respectively.

Significant differences in total CO_2-eq. emissions were observed as a function of GWP time horizon, regardless of the landfill investigated. Given the diversity in gases emitted from landfills including a wide range of NMVOCs, short, as compared to long, GWP time horizons may provide more representative and meaningful climate impact assessments of solid waste landfills. A majority of NMVOC compounds are highly reactive gases, taking part in a number of photochemical reactions over quick timescales (i.e., on the order of seconds to minutes). These photochemical reactions, in turn, affect the atmospheric concentrations and lifetimes of the main GHGs, including methane and nitrous oxide. GHG emission inventories and climate impact assessments targeting solid waste management infrastructure should integrate indirect factors, including stratospheric ozone depletion and secondary organic aerosol effects, as these contributions lead to noticeable reductions in

positive GWP emissions associated with the main GHGs. Excluding negative GWP contributions from the F-gases (e.g., CFCs) and select NMVOCs (e.g., monoterpenes) can lead to overestimation of total CO_2-eq. emissions from landfills, particularly over short operational timescales. Over similar timescales, relying on a 100-yr GWP time horizon can lead to underestimation of climate forcing landfill emissions. These observations are critical to consider in particular for short-term gas emission mitigation measures for landfills, favoring the application of 20-yr GWP time horizons as well as comprehensive analysis of the full range in climate impacts of GHG and NMVOC emissions.

5. Summary and conclusions

This investigation was conducted to provide a comprehensive and systematic analysis of surface emissions and associated time-dependent climate forcing impacts from landfills. Analysis was conducted using 20- and 100-yr time horizons to evaluate climate impacts of both short- and long-lived landfill gases. In the test program, fluxes of 80 gases were determined using ground-based field testing at five sites in California, which collectively contained 13% of the waste in place in active landfills. The gases included: i) anthropogenic GHGs main landfill gas methane and trace gases nitrous oxide and F-gases (13 species) and ii) 65 species of trace non-methane volatile organic compounds categorized under 10 chemical families. Analysis was conducted for all three cover categories (daily, intermediate, and final) used at active landfills. The measured fluxes were converted to whole-site emissions using relative areal extents of different covers at the sites. Direct and indirect climate forcing impacts of the gases were quantified using global warming potential (direct and indirect); atmospheric degradation (direct); tropospheric ozone forming potential (indirect); secondary aerosol forming potential (indirect) and stratospheric ozone depleting potential (indirect) of the gases. Whole-site emissions and direct, indirect, and total (direct + indirect) climate forcing emissions were calculated for both 20- and 100-yr GWP time horizons. Both the magnitude and relative contributions of main and trace gas emissions and direct and indirect emissions to total climate impacts were assessed.

Positive fluxes and emissions were measured for all 80 gases from all three cover categories at all five landfills. Highest fluxes were obtained for GHGs, alkanes, monoterpenes, alcohols, and ketones. Methane flux was higher than the fluxes of the other GHGs and the NMVOCs. Variability of flux was lower for the NMVOCs than the GHGs. Flux varied mainly by cover category decreasing from daily to intermediate to final covers and secondarily by season. Of the three categories of emissions determined, baseline, direct, and indirect, the direct emissions were consistently higher than the baseline and indirect emissions. The direct emissions were essentially positive and high, whereas indirect emissions were mostly negative and low. The ranges for 20-yr and 100-yr direct emissions were 683 to 103,411 and 381 to 37,925 Mg CO_2-eq./yr. The ranges for 20-yr and 100-yr indirect emissions were −3,337 to 189 and −3,768 to 183 Mg CO_2-eq./yr. The ranges for 20-yr and 100-yr total emissions were 680 to 103,600 and 374 to 38,108 Mg CO_2-eq./yr. Direct and indirect emissions were mainly attributed to the high positive radiative forcings of the baseline GHGs (i.e., methane, nitrous oxide, F-gases) and the high ozone depletion potentials of the F-gases, respectively. Baseline and direct emissions were controlled by GHG emissions and indirect emissions were controlled by NMVOCs (e.g., alkanes, alkenes, alcohols, monoterpenes). Within the GHGs, methane contributed most to both baseline and direct emissions. The relative contributions of methane decreased from baseline to direct emissions analysis and relative contributions of the trace GHGs nitrous oxide and in particular F-gases significantly increased due to the comparatively high global warming potentials, particularly of the F-gases. The 20-yr direct and total emissions were consistently higher than the corresponding 100-yr emissions by up to 2.5 times. Inclusion of the indirect effects in the total emissions calculations offset total climate forcing impacts for each landfill, reducing the total emissions by 0.03 to 15%. The effects of indirect emissions were more significant for NMVOCs and 100-yr GWP analysis. Decreasing intermediate cover areas and accelerating transition of these areas to final covers is a viable strategy to mitigate and/or control gas emissions from landfills in particular for short time horizons. Similarly, reducing the areal extent of daily covers has a significant impact on mitigation of total climate forcing landfill emissions.

For complete assessment of landfill impacts on anthropogenic climate drivers, all primary GHGs and trace NMVOCs are recommended to be investigated. Short-term time horizons provide representative estimates of the climate forcing impacts of MSW landfills, as a majority of the atmospheric lifetimes of the landfill gas pollutants and climate drivers are short (i.e., less than 1- to 20-yr lifetime). The 20-yr analysis is appropriate for assessing impacts of current and short-term emissions reduction measures. The 100-yr analysis (with lower total emissions than 20-yr analysis) does not capture immediate or short-term variability in direct and indirect climate forcing impacts and is best-suited for landfill sites where no changes are expected to operational and environmental conditions for extended periods of time and also for closed landfills.

CRediT authorship contribution statement

Derek C. Manheim: Conceptualization, Investigation, Methodology, Software, Writing – original draft, Writing – review & editing. **Nazli Yeşiller:** Conceptualization, Formal analysis, Funding acquisition, Investigation, Methodology, Project administration, Resources, Supervision, Validation, Writing – original draft, Writing – review & editing. **James L. Hanson:** Conceptualization, Data curation, Formal analysis, Funding acquisition, Investigation, Methodology, Project administration, Resources, Supervision, Validation, Visualization, Writing – original draft, Writing – review & editing. **Donald R. Blake:** Data curation, Formal analysis, Funding acquisition, Resources.

Declaration of competing interest

The authors declare the following financial interests/personal relationships which may be considered as potential competing interests: [Derek C. Manheim reports financial support was provided by California Air Resources Board. Derek C. Manheim reports financial support was provided by CalRecycle].

Acknowledgment

This investigation was funded by the California Department of Resources Recycling and Recovery (Contract: DRR16109) and the California Air Resources Board (Contract: 16ISD006). Partial funding was provided by the Global Waste Research Institute. The cooperation of partner landfills is appreciated. Numerous graduate and undergraduate students participated in the field campaigns. Dr. Jean Bogner participated in the field campaigns and analysis of results.

Appendix

Table A1
Characteristics of Gas Constituents.

Chemical Family (Abbr.)	Sources[1]	Chemical Species	Chemical Formula	20-yr DGWP[2]	100-yr DGWP[2]	20-yr IGWP[3]	100-yr IGWP[3]	OFP[4] (g O_3/g species)	SOAP[5] (%)	20-yr $IGWP^6_{ODP}$	100-yr $IGWP^7_{ODP}$
Greenhouse Gases (GHG)	FW, GW	Methane	CH_4	81.2	28	NA	NA	0.014	NA	NA	NA
		Nitrous Oxide	N_2O	273	273	NA	NA	NA	NA	NA	NA
	AppW, C&D, AW	CFC-11	CCl_3F	7430	5560	NA	NA	NA	NA	−2460	−2860
		CFC-12	CCl_2F_2	11,400	11,200	NA	NA	NA	NA	−1210	−2050
		CFC-113	$C_2Cl_3F_3$	12,400	6520	NA	NA	NA	NA	−1450	−2180
		CFC-114	$C_2Cl_2F_4$	8260	9430	NA	NA	NA	NA	−1308.3	−880
		HCFC-21	$CHCl_2F$	575	160	NA	NA	NA	NA	−310	−67.8
		HCFC-22	$CHClF_2$	5690	1960	NA	NA	NA	NA	−98	−98
		HCFC-141b	CCl_2FCH_3	2710	860	NA	NA	NA	NA	−760	−250
		HCFC-142b	$C_2H_3ClF_2$	5510	2300	NA	NA	NA	NA	−320	−160
		HFC-134a	CH_2FCF_3	4140	1260	NA	NA	NA	NA	NA	NA
		HFC-152a	$C_2H_4F_2$	591	164	NA	NA	NA	NA	NA	NA
		HFC-245fa	$CF_3CH_2CHF_2$	3170	962	NA	NA	NA	NA	NA	NA
		HFC-365mfc	$C_4H_5F_5$	2920	914	NA	NA	NA	NA	NA	NA
		Halon-1211	$CBrClF_2$	4920	1930	NA	NA	NA	NA	−18,960	−18,500
Reduced Sulfur Compounds (RSC)	FW, GW, C&D	Carbonyl sulfide	COS	NA	NA	0	0	NA	NA	NA	NA
		Di-methyl sulfide	C_2H_6S	NA	NA	0	0	NA	NA	NA	NA
		Di-methyl disulfide	$C_2H_6S_2$	NA	NA	0	0	NA	NA	NA	NA
		Carbon disulfide	CS_2	NA	NA	0	0	NA	NA	NA	NA
Halogenated Hydrocarbons (HH)	TW, HCW, PW	Chloroform	$CHCl_3$	74.2	20.6	0	0	0.0255	NA	NA	NA
		Methyl chloroform	$C_2H_3Cl_3$	567	161	0	0	0.0052	NA	−990	−310
		Carbon tetrachloride	CCl_4	3810	2200	0	0	NA	NA	−3020	−2610
		Methylene chloride	CH_2Cl_2	40.2	11.2	0	0	0.0491	NA	NA	NA
		Trichloroethylene	C_2HCl_3	0.158	0.044	7.05	2.11	0.746	NA	NA	NA
		Tetrachloroethylene	C_2Cl_4	22.8	6.34	3.13	0.93	0.0373	NA	NA	NA
		Methyl chloride	CH_3Cl	19.9	5.54	1.20	0.36	0.042	NA	NA	NA
		Bromomethane	CH_3Br	8.74	2.43	1.92	0.60	0.0206	NA	−4280	−1210
		Dibromomethane	CH_2Br_2	5.45	1.51	0	0	NA	NA	NA	NA
		Bromodichloromethane	$CHBrCl_2$	NA	NA	0	0	NA	NA	NA	NA
		Bromoform	$CHBr_3$	NA	NA	0	0	NA	NA	NA	NA
		Chloroethane	C_2H_5Cl	1.73	0.481	4.37	1.31	0.343	NA	NA	NA
		1,2-Dichloroethane	$C_2H_4Cl_2$	4.68	1.3	0	0	0.228	NA	NA	NA
		1,2-Dibromoethane	$C_2H_4Br_2$	3.67	1.02	0	0	0.108	NA	NA	NA
Organic (Alkyl) Nitrates (ON)	OBP	Methyl Nitrate	CH_3NO_3	NA	NA	0	0	NA	NA	NA	NA
		Ethyl Nitrate	$C_2H_5NO_3$	NA	NA	1.24	0.33	NA	NA	NA	NA
		Isopropyl nitrate	$C_3H_7NO_3$	NA	NA	1.88	0.52	NA	NA	NA	NA
		N-propyl nitrate	$C_3H_7HO_3$	NA	NA	6.28	1.90	NA	NA	NA	NA
		2-butyl nitrate	$C_4H_9NO_3$	NA	NA	6.37	1.89	NA	NA	NA	NA
Alkanes (Alk)	PW, HCW, CW, PaW, PapW	Ethane	C_2H_6	1.57	0.437	18.60	5.90	0.321	NA	NA	NA
		Propane	C_3H_8	0.072	0.02	18.30	5.80	0.563	NA	NA	NA
		i-Butane	C_4H_{10}	NA	NA	14.12	4.44	1.3	NA	NA	NA
		n-Butane	C_4H_{10}	0.022	0.006	10.50	3.20	1.33	NA	NA	NA
		i-Pentane	C_5H_{12}	NA	NA	15.99	5.05	1.65	NA	NA	NA
		n-Pentane	C_5H_{12}	NA	NA	20.70	6.60	1.56	NA	NA	NA
		n-Hexane	C_6H_{14}	NA	NA	21.30	6.80	1.55	NA	NA	NA
		n-Undecane	$C_{11}H_{24}$	NA	NA	11.09	3.40	0.849	2.5	NA	NA
Alkenes (Alke)	PW, HCW, CW, PaW, PapW	Ethene	C_2H_4	NA	NA	10.80	3.30	8.64	0.3	NA	NA
		Propene	C_3H_6	NA	NA	11.70	3.60	10.8	NA	NA	NA
		1-Butene	C_4H_8	NA	NA	7.05	2.11	9.3	NA	NA	NA
		i-Butene	C_4H_8	NA	NA	4.95	1.45	5.37	NA	NA	NA
		trans-2-butene	C_4H_8	NA	NA	4.88	1.43	12.5	NA	NA	NA
		cis-2-butene	C_4H_8	NA	NA	4.70	1.37	12.2	NA	NA	NA
		1-Pentene	C_5H_{10}	NA	NA	6.85	2.04	6.92	NA	NA	NA
		Isoprene	C_5H_8	NA	NA	3.88	1.10	9.71	0.6	NA	NA
Aldehydes/ Alkynes (Ald/Alky)	PW, HCW, CW, PaW, PapW	Ethyne	C_2H_2	NA	NA	7.38	2.22	0.944	NA	NA	NA
		Acetaldehyde	C_2H_4O	NA	NA	2.44	0.64	6.07	NA	NA	NA
		Butanal	C_4H_8O	NA	NA	5.49	1.62	5.73	NA	NA	NA
Aromatic Hydrocarbons (Ar)	FW, HCW, CW, PCPW, HSPW, PW, PaW, TW, FuW	Benzene	C_6H_6	NA	NA	3.88	1.10	0.787	2.6	NA	NA
		Toluene	C_7H_8	NA	NA	3.88	1.10	4.02	5.4	NA	NA
		Ethylbenzene	C_8H_{10}	NA	NA	10.86	3.34	3.11	5.4	NA	NA
		m + p-Xylene	C_8H_{10}	NA	NA	10.20	3.11	4.3	3.15	NA	NA
		o-Xylene	C_8H_{10}	NA	NA	10.12	3.08	7.17	5	NA	NA
		i-Propylbenzene	C_9H_{12}	NA	NA	0	0	2.58	4	NA	NA
		n-Propylbenzene	C_9H_{12}	NA	NA	0	0	2.15	1.6	NA	NA
		3-Ethyltoluene (M)	C_9H_{12}	NA	NA	0	0	6.7	6.3	NA	NA
		4-Ethyltoluene (P)	C_9H_{12}	NA	NA	10.90	3.34	4.28	2.5	NA	NA
		2-Ethyltoluene (O)	C_9H_{12}	NA	NA	11.07	3.39	5.33	5.6	NA	NA
		1–3-5-Trimethylbenzene	C_9H_{12}	NA	NA	9.15	2.77	9.35	2.9	NA	NA

(*continued on next page*)

Table A1 (*continued*)

Chemical Family (Abbr.)	Sources[1]	Chemical Species	Chemical Formula	20-yr DGWP[2]	100-yr DGWP[2]	20-yr IGWP[3]	100-yr IGWP[3]	OFP[4] (g O_3/g species)	SOAP[5] (%)	20-yr $IGWP^6_{ODP}$	100-yr $IGWP^7_{ODP}$
		1,2,3-Trimethylbenzene	C_9H_{12}	NA	NA	8.23	2.46	9.86	3.6	NA	NA
		1,2,4-Trimethylbenzene	C_9H_{12}	NA	NA	8.27	2.47	7.88	2	NA	NA
Monoterpenes (Mon)	GW, PCPW, C&D, HCW, HSPW	α-pinene	$C_{10}H_{16}$	NA	NA	2.54	0.70	4.02	30	NA	NA
		β-pinene	$C_{10}H_{16}$	NA	NA	2.54	0.70	3.47	30	NA	NA
		Limonene	$C_{10}H_{16}$	NA	NA	2.54	0.70	4.06	NA	NA	NA
Alcohols (Alc)	FW, HCW, PCPW, HSPW	Methanol	CH_4O	NA	NA	5.50	1.60	0.668	NA	NA	NA
		Ethanol	C_2H_6O	NA	NA	6.27	1.88	1.79	NA	NA	NA
		Isopropanol	C_3H_8O	NA	NA	7.67	2.31	0.644	NA	NA	NA
		2-Butanol	$C_4H_{10}O$	NA	NA	8.84	2.69	1.52	NA	NA	NA
Ketones (Ket)	FW, HCW, PCPW, HSPW	Acetone	C_3H_6O	0.5	0.5	1.15	0.30	0.343	NA	NA	NA
		Butanone	C_4H_8O	NA	NA	4.81	1.39	1.53	NA	NA	NA
		Methylisobutylketone	$C_6H_{12}O$	NA	NA	7.54	2.27	3.81	NA	NA	NA

[1]Adapted from Nair et al. (2019). FW = food wastes; PapW = paper wastes; GW = green wastes (i.e., yard trimmings); C&D = construction and demolition wastes (e.g., concrete, metal, wood, drywall); AW = auto-wastes; TW = textile wastes (i.e., clothes, carpet); HCW = household cleaning wastes; PW = plastic wastes; OBP = oxidation byproduct of NMVOCs in the landfill environment; CW = cooking wastes (i.e., charcoal, propane fuels); PCPW = personal care product wastes (i.e., shampoo, toothpaste); HSPW = household spray product wastes (i.e., air fresheners); PaW = paint wastes; FuW = furniture wastes; AppW = appliance wastes.
[2]All DGWP values obtained from IPCC (2021).
[3]Select IGWP values obtained from Johnson and Derwent (1996), Collins et al. (2002), Hodnebrog et al. (2018), and all other IGWP values were interpolated based on atmospheric reactivity.
[4]Carter (2010).
[5]Grosjean and Seinfeld (1989).
[6]Daniel et al. (1995).
[7]WMO (2018).
[NA]Not available and/or reported from the literature.

References

Abichou, T., Chanton, J., Powelson, D., Fleiger, J., Escoriaza, S., Lei, Y., Stern, J., 2006. Methane flux and oxidation at two types of intermediate landfill covers. Waste Manag. 26, 1305–1312. https://doi.org/10.1016/j.wasman.2005.11.016.

Atkinson, R., Arey, J., 2003. Gas-phase tropospheric chemistry of biogenic volatile organic compounds: A review. Atmos. Environ. 37, 197–219. https://doi.org/10.1016/S1352-2310(03)00391-1.

Barlaz, M.A., Green, R.B., Chanton, J.P., Goldsmith, C.D., Hater, G.R., 2004. Evaluation of a biologically active cover for mitigation of landfill gas emissions. Environ. Sci. Tech. 38, 4891–4899. https://doi.org/10.1021/es049605b.

Beck, H.E., Zimmermann, N.E., McVicar, T.R., Vergopolan, N., Berg, A., Wood, E.F., 2018. Present and future köppen-geiger climate classification maps at 1-km resolution. Sci. Data 5, 180214. https://doi.org/10.1038/sdata.2018.214.

Boucher, O., Friedlingstein, P., Collins, B., Shine, K.P., 2009. The indirect global warming potential and global temperature change potential due to methane oxidation. Environ. Res. Lett. 4, 044007 https://doi.org/10.1088/1748-9326/4/4/044007.

California Air Resources Board (CARB), 2020. *California Greenhouse Gas Emissions for 2000 to 2017, Trends of Emissions and Other Indicators, 2019 Edition*. https://ww3.arb.ca.gov/cc/inventory/pubs/reports/2000_2017/ghg_inventory_trends_00-17.pdf.

Carter, W., 2010. Updated maximum incremental reactivity scale and hydrocarbon bin reactivities for regulatory applications. California Air Resources Board. http://ww2.arb.ca.gov/sites/default/files/barcu/regact/2009/mir2009/mir10.pdf.

Chanton, J., Abichou, T., Langford, C., Spokas, K., Hater, G., Green, R., Goldsmith, D., Barlaz, M.A., 2011. Observations on the methane oxidation capacity of landfill soils. Waste Manag. 31, 914–925. https://doi.org/10.1016/j.wasman.2010.08.028.

Christensen, T.H., Kjeldsen, P., Lindhart, B., 1996. Gas-generating processes in landfills. In: Christensen, T.H., Cossu, R., Stegmann, R. (Eds.), Landfilling of Waste: Biogas, 1st Edition. Taylor and Francis, London, pp. 39–50.

Collins, W.J., Derwent, R.G., Johnson, C.E., Stevenson, D.S., 2002. The oxidation of organic compounds in the troposphere and their global warming potentials. Clim. Change 52, 453–479. https://doi.org/10.1023/A:1014221225434.

Daniel, J.S., Solomon, S., Albritton, D.L., 1995. On the evaluation of halocarbon radiative forcing and global warming potentials. J. Geophys. Res. Atmos. 100, 1271–1285. https://doi.org/10.1029/94JD02516.

Grosjean, D., Seinfeld, J.H., 1989. Parameterization of the formation potential of secondary organic aerosols. Atmos. Environ. 1967 (23), 1733–1747. https://doi.org/10.1016/0004-6981(89)90058-9.

Hanson, J. L., Yesiller, N., and Kendall, L. A., 2005. Integrated Temperature and Gas Analysis at a Municipal Solid Waste Landfill. In Proceedings of the 16th International Conference on Soil Mechanics and Geotechnical Engineering, 2265–2268. Doi: 10.3233/978-1-61499-656-9-2265.

Hanson, J. L., Yesiller, N., Howard, K. A., Liu, W. L., Cooper, S. P., 2006. Effects of Placement Conditions on Decomposition of Municipal Solid Wastes in Cold Regions. In Proceedings of 13th International Conference on Cold Regions Engineering, 1–13. Doi: 10.1061/40836(210)48.

Hanson, J. L., Yesiller, N., and Manheim, D. C., 2020. *Estimation and Comparison of Methane, Nitrous Oxide, and Trace Volatile Organic Compound Emissions and Gas Collection System Efficiencies in California Landfills*. Final Report Submitted to CalRecycle and CARB. https://ww2.arb.ca.gov/sites/default/files/2020-06/CalPoly%20LFG%20Flux%20and%20Collection%20Efficiencies%203-30-2020.pdf.

Hanson J. L., Manheim, D. C., and Yesiller, N., 2023b. Climate Impacts of Trace Gas Emissions from Solid Waste Landfills. In Geo-Congress 2023: Soil Improvement, Geoenvironment, and Sustainability, 201–210. Doi: 10.1061/9780784484661.021.

Hanson, J.L., Manheim, D.C., Yeşiller, N., 2023. Geoenvironmental assessment of climate impacts from landfill gas emissions. Soils Found. 63, 1–24. https://doi.org/10.1016/j.sandf.2023.101279.

Hodnebrog, Ø., Dalsøren, S.B., Myhre, G., 2018. Lifetimes, direct and indirect radiative forcing, and global warming potentials of ethane (C_2H_6), propane (C_3H_8), and butane (C_4H_{10}). Atmos. Sci. Lett. 19, e804.

IPCC, 2021. Summary for Policymakers, in: Masson-Delmotte, V., Zhai, P., Pirani, A., Connors, S. L., Péan, C., Berger, S., Caud, N., Chen, Y., Goldfarb, L., Gomis, M. I., Huang, M., Leitzell, K., Lonnoy, E., Matthews, J. B. R., Maycock, T. K., Waterfield, T., Yelekçi, O. R. Yu and B. Zhou (Eds.), Climate Change 2021: The Physical Science Basis. Contribution of Working Group I to the Sixth Assessment Report of the Intergovernmental Panel on Climate Change. Cambridge University Press.

Johnson, C.E., Derwent, R.G., 1996. Relative radiative forcing consequences of global emissions of hydrocarbons, carbon monoxide and NOx from human activities estimated with a zonally-averaged two-dimensional model. Clim. Change 34, 439–462. https://doi.org/10.1007/BF00139301.

Kaza, S., Yao, L., Bhada-Tata, P., Woerden, F.V., 2018. What a waste 2.0: A global snapshot of solid waste management to 2050. World Bank Publications.

Majumdar, D., Srivastava, A., 2012. Volatile organic compound emissions from municipal solid waste disposal sites: A case study of mumbai, india. J. Air Waste Manag. Assoc. 62, 398–407. https://doi.org/10.1080/10473289.2012.655405.

Manheim, D.C., Yeşiller, N., Hanson, J.L., 2021a. Gas emissions from municipal solid waste landfills: A comprehensive review and analysis of global data. J. Indian Inst. Sci. 101, 625–657. https://doi.org/10.1007/s41745-021-00234-4.

Manheim, D.C., Yesiller, N., Hanson, J.L., 2021b. Climate change effects of gases from municipal solid waste landfills. JGS Special Publication 9, 142–147. https://doi.org/10.3208/jgssp.v09.cpeg035.

Matlab, 2022. MATLAB and statistics toolbox release 2022. The MathWorks Inc, Natick, Massachusetts, United States.

McGillen, M.R., Carter, W.P.L., Mellouki, A., Orlando, J.J., Picquet-Varrault, B., Wallington, T.J., 2020. Database for the kinetics of the gas-phase atmospheric reactions of organic compounds. Earth Syst. Sci. Data 12, 1203–1216. https://doi.org/10.5194/essd-12-1203-2020.

Mønster, J., Kjeldsen, P., Scheutz, C., 2019. Methodologies for measuring fugitive methane emissions from landfills – a review. Waste Manag. 87, 835–859. https://doi.org/10.1016/j.wasman.2018.12.047.

Nair, A.T., Senthilnathan, J., Nagendra, S.M.S., 2019. Emerging perspectives on VOC emissions from landfill sites: impact on tropospheric chemistry and local air quality. Process Saf. Environ. Prot. 121, 143–154. https://doi.org/10.1016/j.psep.2018.10.026.

Prinn, R.G., Weiss, R.F., Arduini, J., Arnold, T., DeWitt, H.L., Fraser, P.J., Ganesan, A.L., Gasore, J., Harth, C.M., Hermansen, O., Kim, J., Krummel, P.B., Li, S., Loh, Z.M.,

Lunder, C.R., Maione, M., Manning, A.J., Miller, B.R., Mitrevski, B., Zhou, L., 2018. History of chemically and radiatively important atmospheric gases from the advanced global atmospheric gases experiment (AGAGE). Earth Syst. Sci. Data 10, 985–1018. https://doi.org/10.5194/essd-10-985-2018.

Rolston, D.E., 1986. 47-gas flux. In: Klute, A. (Ed.), Methods of Soil Analysis: Part I, Physical and Mineralogical Methods, 2nd Edition. American Society of Agronomy/ Soil Science Society of America, Madison, WI, pp. 1103–1119.

Saunois, M., et al., 2020. The global methane budget 2000–2017. Earth Syst. Sci. Data 12, 1561–1623. https://doi.org/10.5194/essd-12-1561-2020.

Scheutz, C., Kjeldsen, P., 2003. Capacity for biodegradation of CFCs and HCFCs in a methane oxidative counter-gradient laboratory system simulating landfill soil covers. Environ. Sci. Tech. 37, 5143–5149. https://doi.org/10.1021/es026464+.

Tchobanoglous, G., Theisen, H., Vigil, S., 1993. Integrated solid waste management: Engineering principles and management issues. McGraw-Hill, New York.

Unger, N., 2014. On the role of plant volatiles in anthropogenic global climate change. Geophys. Res. Lett. 41, 8563–8569. https://doi.org/10.1002/2014GL061616.

USEPA, 2022. *AirData: Air Quality Data Collected at Outdoor Monitors Across the US*. https://www.epa.gov/outdoor-air-quality-data.

USEPA, 2023. *Inventory of US Greenhouse Gas Emissions and Sinks (1990-2021)*. https://www.epa.gov/system/files/documents/2023-04/US-GHG-Inventory-2023-Main-Text.pdf.

World Meteorological Organization (WMO), 2018. Chapter 6: Scenarios and Information for Policy Makers, in: Carpenter, L. J. and Daniel, J. S. (Eds.), Scientific Assessment of Ozone Depletion: 2018, Global Ozone Research and Monitoring Project–Report No. 58. Geneva, Switzerland.

Wuebbles, D.J., Grossman, A.S., Tamaresis, J.S., Patten, J., Jain, A., and Grant, K.A., 1994. *Indirect Global Warming Effects of Ozone and Stratospheric Water Vapor Induced by Surface Methane Emission (No. UCRL-ID-118061)*. Lawrence Livermore National Lab, Livermore, CA (United States). Doi: 10.2172/10182802.

Yeşiller N, Hanson, J.L., Manheim, D.C., Limpert, A.D., 2019. Emissions of High Global Warming Potential and Ozone Depleting Substance Gases from California Landfills. In Proceedings Geo-Environmental Engineering (GEE 2019), 1–7.

Yeşiller, N., Hanson, J.L., Sohn, A.H., Bogner, J.E., Blake, D.R., 2018. Spatial and temporal variability in emissions of fluorinated gases from a california landfill. Environ. Sci. Tech. 52, 6789–6797. https://doi.org/10.1021/acs.est.8b00845.